

The Distance to the Magellanic Clouds

B o h d a n P a c z y ń s k i

Princeton University Observatory, Princeton, NJ 08544-1001, USA
e-mail: bp@astro.princeton.edu

ABSTRACT

The distance to LMC and SMC is a subject of controversy, with the difference between the extreme values in distance moduli exceeding 0.5 mag. While currently the best calibrated method is based on red clump giants, and the near future improvement is most likely to come from detached eclipsing binaries, the ultimate goal is to have a purely geometrical determination. The best prospect will be to use relatively wide binary stars, for which spectroscopic orbits will be obtained with large ground based telescopes, and astrometric orbits will be obtained either with SIM, or with future ground based interferometers. A preliminary list of 25 candidate systems is presented. It is based on OGLE catalogs of BVI photometry.

Key words: *galaxies: Magellanic Clouds - stars: binaries: spectroscopic - stars: binaries: visual - stars: distances*

1 Introduction

The distance to the Large Magellanic Cloud is not agreed upon. A recent compilation of the values of distance modulus published in 1998 and 1999 (Gibson 1999) cover a range from 18.07 to 18.74, which corresponds to a factor 1.36 in the distance. An attempt to harmonize the distance scale based on RR Lyrae variables and red clump giants, the two best calibrated indicators, gives a range 18.24 - 18.44 (Popowski 2001). I think the current empirical calibration of the red clump giants is the most reliable, and this gives 18.24 ± 0.08 (Udalski 2000), but the issue is far from being settled.

In the near future the most reliable results will be obtained with analysis of detached eclipsing binaries. A very good description of method, and many historical references dating from 1910, can be found in Kruszewski and Semeniuk (1999). The method was applied by Lacy (1979) to several dozens nearby systems, and the distances he obtained have been verified with the Hipparcos parallaxes (Ribas et al. 1998, Semeniuk 2000). A much better calibration will be provided by the future Full-sky Astrometric Mapping Explorer (FAME, Horner et al. 1999, Semeniuk 2001). However, even

today this method provides the LMC distance which is competitive with the best alternatives. The first modern determination of the LMC distance modulus based on eclipsing binaries were by Bell et al. (1991) and Bell et al. (1993), who used HV2226 and HV5936 to obtain 18.6 ± 0.3 and 18.1 ± 0.3 , respectively. More recently HV 2274 was observed by Guinan and his collaborators, and they obtained for the distance modulus values 18.54 ± 0.08 , 18.42 ± 0.07 , and 18.30 ± 0.07 (Guinan et al. 1997, 1998a, 1998b, respectively). The same data but different analysis of the interstellar reddening provided somewhat different values: 18.22 ± 0.13 (Udalski et al. 1998b) and 18.40 ± 0.07 (Nelson et al. 2000). Finally, Fitzpatrick et al. (2000) obtained 18.31 ± 0.09 using HV982. While the agreement between various determinations is not perfect, they all are in a reasonable agreement with the ‘short’ distance scale to the LMC.

While I expect that there will be a major improvement in the distance determinations using detached eclipsing binaries, and the errors in the distance modulus will be reduced to 0.05 mag, or even less, it is far from clear that the proponents of a different distance value will be convinced. Ultimately, it would be important to obtain a 1% distance using some purely geometric method. This will not be easy, as even if the Space Interferometry Mission (SIM, Allen et al. 1997) achieves astrometric accuracy of $1 \mu s$, this will translate into 5% accuracy for the distance determination. While in principle the accuracy could be improved by measuring parallaxes to many stars in the LMC, it is not likely that systematic errors will be reduced so much as to make it practical.

In the following section I present an outline of a very traditional and purely geometrical method for distance determination based on a combination of astrometry and spectroscopy of visual binaries. In the subsequent section I present a list of candidate objects, selected from the published OGLE catalogs of BVI photometry for over 7 million stars in the LMC (Udalski et al. 2000), and over 2 million stars in the SMC (Udalski et al. 1998a). Finally, I outline an observational approach to the selection of the best systems.

2 Geometric Distance to the Magellanic Clouds

The simplest and best known geometrical method for distance determination is the traditional parallax. Unfortunately, at the LMC distance even SIM will be able to perform 5% measurement, at best. Fortunately, there is an-

other, almost equally traditional method, based on visual binaries. Combining astrometric and spectroscopic orbits provides 1% distances and masses. Two good examples are ι Pegasi (Boden et al. 1999a) and 64 Piscium (Boden et al. 1999b). This method is likely to settle the controversy over Pleiades distance by determining the orbit of Atlas (Pan et al. 1999).

A great advantage of visual binary method over the parallax is that only small angle relative astrometry is needed. Also, binary orbits may be much larger than 1 AU, making it possible to reach farther with excellent accuracy. One problem is the need to resolve the binary, at least in the conventional use of the binary method. This is a serious problem at the LMC distance of ~ 50 kpc. For a binary in a circular orbit the angular separation is given as

$$\theta = 0.25 \text{ mas} \left(\frac{P_{orb}}{10 \text{ yr}} \right)^{2/3} \left(\frac{M_1 + M_2}{20 M_\odot} \right)^{1/3}, \quad \text{for } d = 50 \text{ kpc.} \quad (1)$$

An orbital period of ~ 10 years is about as long as acceptable, considering rapid progress of technology. The binary HV2274 has the total mass of $23.5 M_\odot$ (Guinan et al. 1998b), and the apparent magnitude $V = 14.16$ (Udalski et al. 1998b), hence the mass scaling adopted in the eq. (1) is reasonable. There are two problems with an application of visual binary method to LMC distance determination: 0.25 mas is too small an angle, and at $V \approx 14$ mag a binary is too faint for current optical and infrared interferometers. However, it is not unreasonable to expect that within the next 5 or 10 years such a binary will be within reach of future ground based instruments.

There another possibility: to use SIM do perform 1 micro-arc-second astrometry on the light centroid of a visual binary. With the expected ~ 10 mas angular resolution SIM could not resolve the binary but it could determine the motion of the light centroid with an accuracy better than 1%. To make this useful we have to select visual binaries made of two diverse components: one very hot and blue, the other very cool and red, and to take advantage of the broad spectral response of the SIM, with many filters covering wavelengths in the range 0.4–0.8 microns, approximately. The location of the light centroid would be close to the hot star in the blue, and close to the cool star in the near infrared. Of course, to be feasible, this approach requires us to decompose the binary spectrum into two components, and to determine the luminosity ratio of the two stars as a function of wavelength. While this is not an easy task, there is no obvious reason for it to be impossible to accomplish. In fact it should be done from the ground prior to any attempt to put a candidate binary on the SIM target list.

Note, that Hipparcos discovered many new visual unresolved binaries by measuring periodic variations in the position of their light centroid (Mignard 1998, and references therein).

For any of the two proposed approaches: either the resolution of an LMC binary with a future ground based interferometer, or the astrometry of the light centroid variations with the future SIM, it is necessary to identify suitable binaries and to determine accurate spectroscopic orbits. With the target stars brighter than 14 mag the determination of accurate radial velocity curve should not be a problem. The candidate stars are selected from the OGLE catalogs of millions of stars in the next section.

3 Candidate Binaries

Udalski et al. (1998a, 2000) published BVI photometry for over 2 million SMC stars, and over 7 million LMC stars, respectively. The results for the SMC and LMC are available over the Internet at:

[http://bulge.princeton.edu/~ ogle/ogle2/bvi_maps.html](http://bulge.princeton.edu/~ogle/ogle2/bvi_maps.html)

http://bulge.princeton.edu/~ ogle/ogle2/lmc_maps.html

and at:

[http://www.astrouw.edu.pl/~ ftp/ogle/ogle2/bvi_maps.html](http://www.astrouw.edu.pl/~ftp/ogle/ogle2/bvi_maps.html)

[http://www.astrouw.edu.pl/~ ftp/ogle/ogle2/lmc_maps.html](http://www.astrouw.edu.pl/~ftp/ogle/ogle2/lmc_maps.html)

The stars selected for analysis were brighter than $V = 14$ mag, and had good photometry in all three bands: B, V, and I. There were 810 such stars in the SMC, and 1127 in the LMC. They are shown in Fig. 1 and Fig. 2 in $(V - I) - (B - V)$ color-color diagrams, and in Fig. 3 and Fig. 4 in color-magnitude diagrams. The diagonal lines in Fig. 1 and Fig. 2 correspond to the relation:

$$(B - V) = \frac{7}{6} (V - I) - 0.5. \quad (2)$$

The open circles located below this line are the stars which have an excess of light in the B and I bands, i.e. these are the candidates for unresolved blue-red binaries. They are all listed in Table 1, in which the second columns give the OGLE field number, and the third columns the star number within the corresponding fields. All other columns are self-explanatory. Finding charts for all the candidate binaries are shown in Fig. 5 and Fig. 6. The candidate is located at the center of each square panel, which is 1,000 pixels on its side, corresponding to $7'$ in the sky.

4 Discussion

The candidates listed in Table 1 have to be verified spectroscopically for the presence of composite spectra. The next step is more time consuming: for every star with a composite spectrum the two radial velocity curves have to be determined. Some genuine binaries will have periods too short, and hence angular separations too small to be of interest. Others will have periods too long to be of interest. Hopefully, there will be several objects in the period range of 5 – 15 years, which might be considered to be optimal for distance determination.

The list of candidate binaries will increase as OGLE upgrades to a large mosaic CCD camera, and multi-band photometry will become available for full SMC and LMC, not just for their central regions. Also, photometry for the stars which are brighter than the saturation limit apparent in Fig. 3 and Fig. 4 should be searched for possible candidates.

Acknowledgments. This work was supported with the NSF grants AST-9819787 and AST-9820314. It is a great pleasure to acknowledge that all figures were made using the SM plotting package provided by R. H. Lupton.

REFERENCES

- Allen, R., Shao, M., and Patterson, D. 1997, *Proc. SPIE*, **2871**, 504.
 Bell, S. A. et al. 1991, *MNRAS*, **250**, 119.
 Bell, S. A. et al. 1993, *MNRAS*, **265**, 1047.
 Boden, A. F. et al. 1999a, *Astrophys. J.*, **515**, 356.
 Boden, A. F. et al. 1999b, *Astrophys. J.*, **527**, 360.
 Fitzpatrick, E. L. et al. 2000, astro-ph/0010526.
 Gibson, B. K. 1999, astro-ph/9910574.
 Guinan, E. F. et al 1997, *AAS*, **191**, 0313.
 Guinan, E. F. et al. 1998a, astro-ph/9809132v1.
 Guinan, E. F. et al. 1998b, *Astrophys. J. Letters*, **509**, L21.
 Horner, S. D. et al. 1991, astro-ph/9907213.
 Lacy, C. H. 1979, *Astrophys. J.*, **228**, 817.
 Kruszewski, A., and Semeniuk, I. 1999, *Acta Astron.*, **49**, 561.
 F. Mignard, F. 1998, in: *Highlights of Astronomy*, **Vol. 11A**, **JD 14 of the XXIIIrd General Assembly of the IAU**, Ed. J. Andersen. Kluwer Academic Publishers, 1998, p. 539.
 Nelson, C. A. et al. 2000, *Astron. J.*, **119**, 1205.
 Pan, X. P., Shao, M., and Kulkarni, S. 1999, *AAS*, **195**, 132.03.
 Popowski, P. 2001, *MNRAS*, **321**, 502.
 Ribas, I. et al. 1998, *Astron. Astrophys.*, **330**, 600.

- Semeniuk, I. 2000, *Acta Astron.*, **50**, 381.
Semeniuk, I. 2001, astro-ph/0103511.
Udalski, A. 2000, *Astrophys. J. Letters*, **531**, L25.
Udalski, A. et al. 1998b, *Astrophys. J. Letters*, **509**, L25.
Udalski, A. et al. 1998a, *Acta Astron.*, **48**, 147.
Udalski, A. et al. 2000, *Acta Astron.*, **50**, 307.

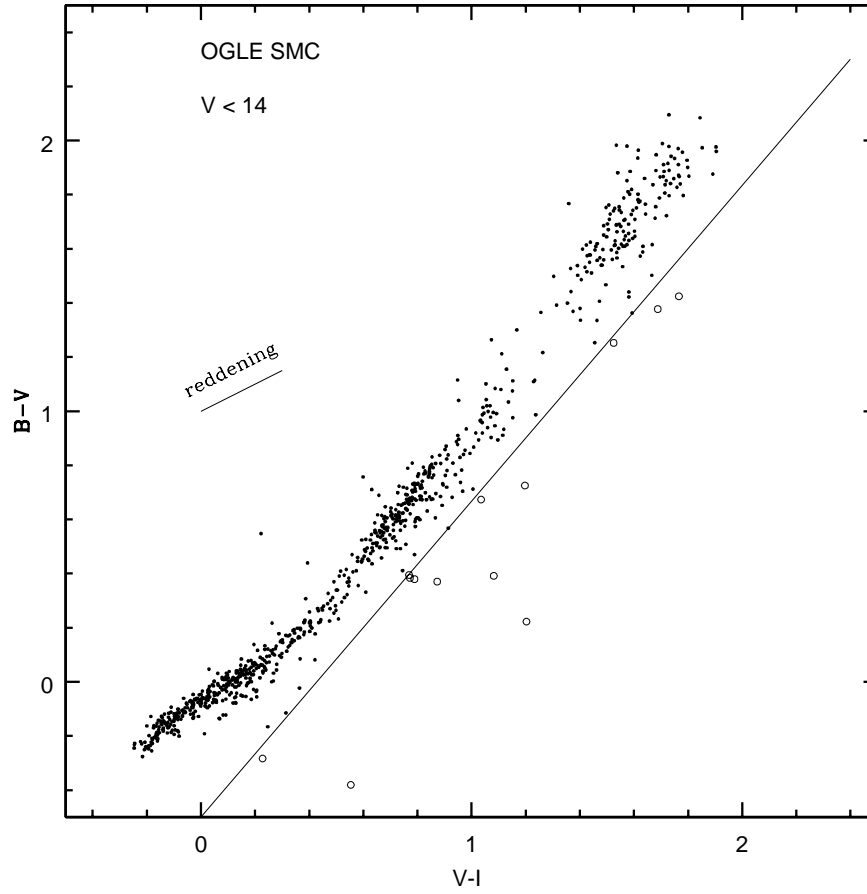


Fig. 1. Color-color diagram for 810 OGLE stars in the SMC that are brighter than $V=14$ mag. The diagonal line is given by the eq. (2). The stars indicated with open circles have an excess of B and I light, and are candidates for blue-red unresolved binaries. A reddening vector is shown.

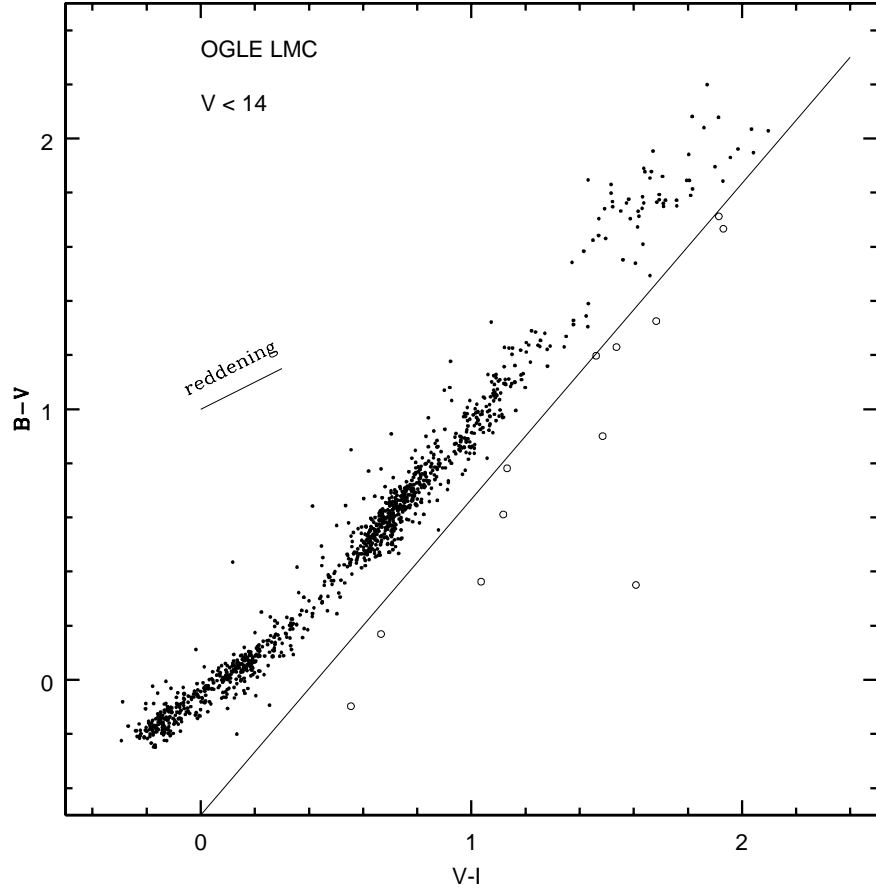


Fig. 2. Color-color diagram for 1127 OGLE stars in the LMC that are brighter than $V = 14$ mag. The diagonal line is given by the eq. (2). The stars indicated with open circles have an excess of B and I light, and are candidates for blue-red unresolved binaries. A reddening vector is shown.

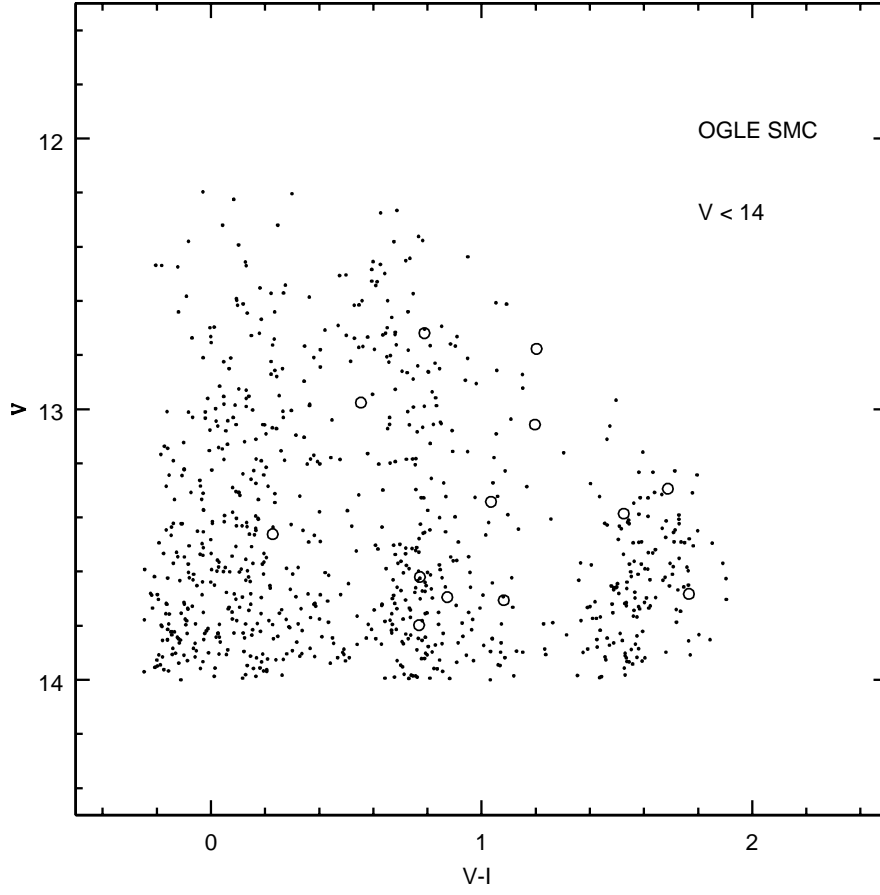


Fig. 3. Color-magnitude diagram for 810 OGLE stars in the SMC that are brighter than $V = 14$ mag. The stars indicated with open circles have an excess of B and I light, and are candidates for blue-red unresolved binaries.

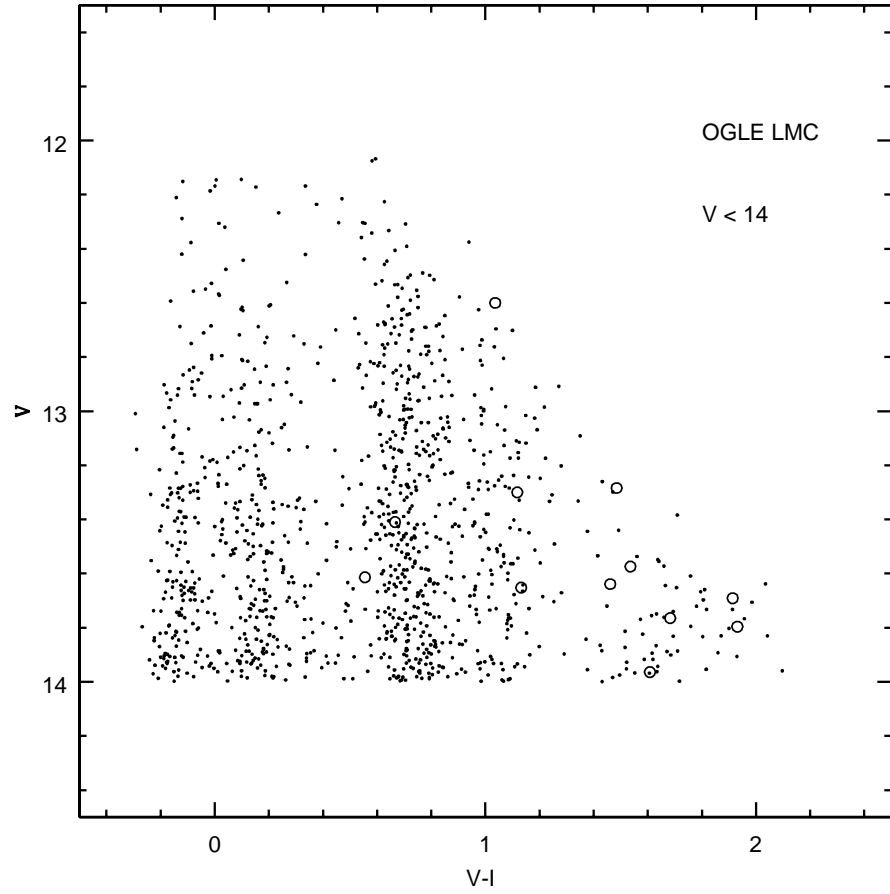


Fig. 4. Color-magnitude diagram for 1127 OGLE stars in the LMC that are brighter than $V = 14$ mag. The stars indicated with open circles have an excess of B and I light, and are candidates for blue-red unresolved binaries.

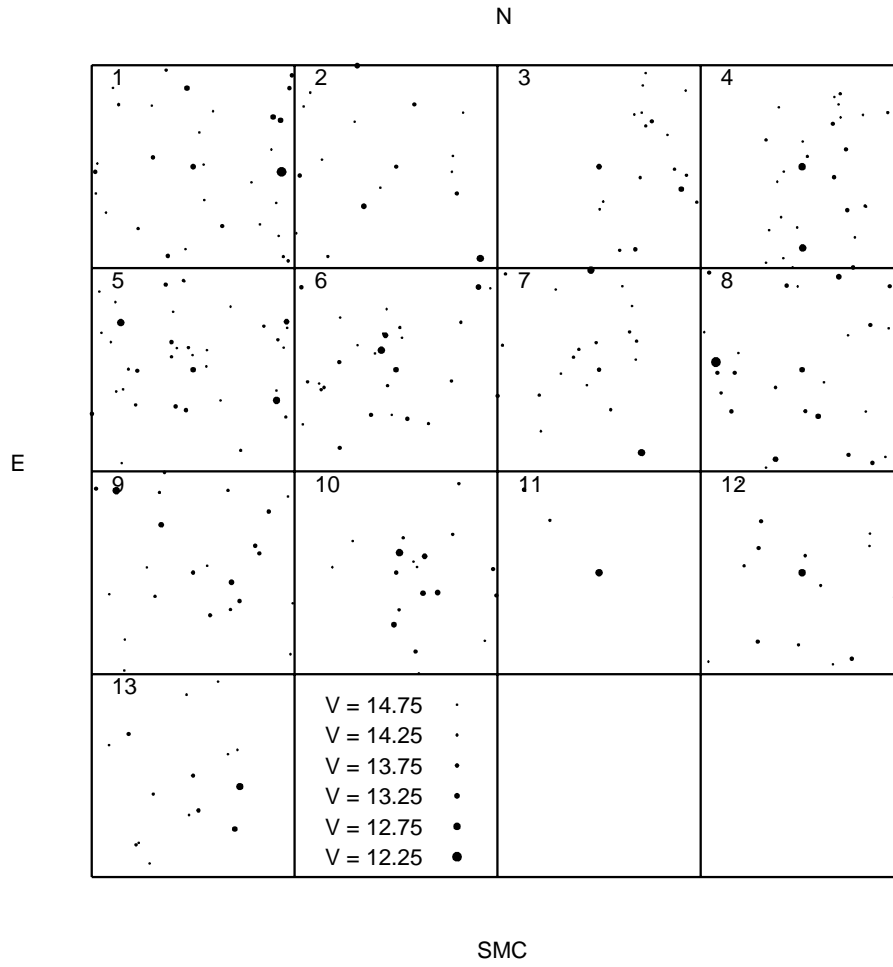


Fig. 5. Finding charts for 13 candidate blue-red unresolved binaries in the SMC. Each square is $7'$ on a side.

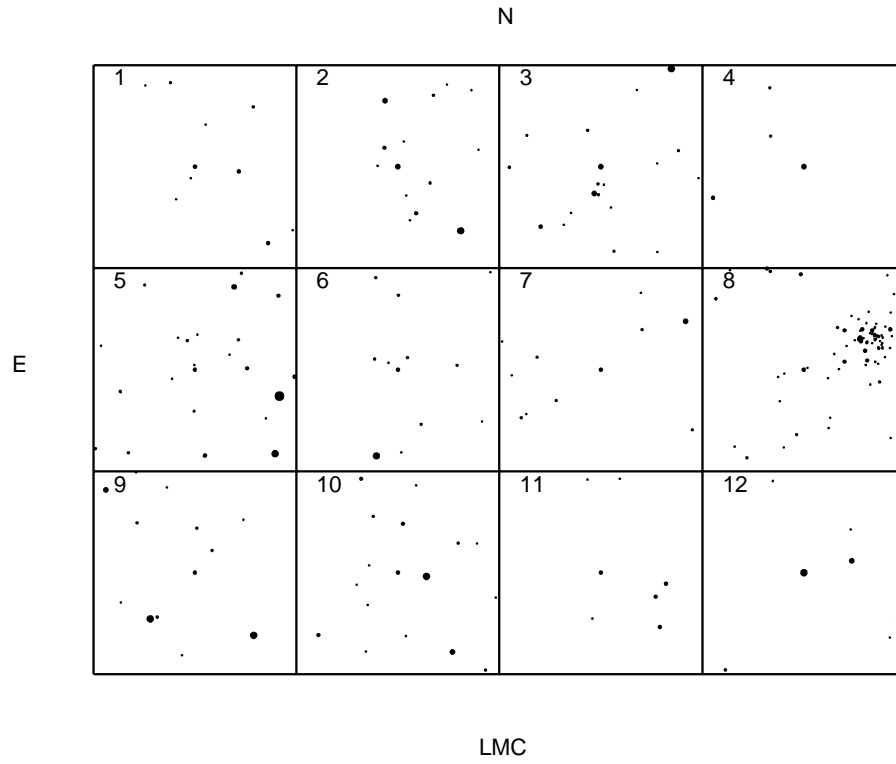


Fig. 6. Finding charts for 12 candidate blue-red unresolved binaries in the LMC. Each square is $7'$ on a side.

Table 1
Candidate binaries in the SMC

	field	number	RA	DEC	V	B-V	V-I
1	4	16915	0:47:08.72	-73:14:11.5	13.057	0.725	1.197
2	5	19933	0:50:32.09	-72:52:09.3	13.695	0.370	0.873
3	6	17257	0:51:22.85	-73:15:41.8	13.462	-0.283	0.228
4	6	35446	0:51:45.43	-73:04:59.7	12.719	0.379	0.789
5	6	10522	0:52:19.06	-73:09:22.7	13.342	0.673	1.035
6	6	50956	0:53:44.49	-72:33:19.0	13.294	1.377	1.688
7	6	11169	0:54:09.53	-72:41:42.9	13.706	0.392	1.082
8	9	14255	1:02:37.90	-72:35:54.4	13.386	1.252	1.525
9	10	545	1:05:10.31	-72:16:44.4	13.683	1.425	1.766
10	11	53227	1:07:04.55	-72:25:51.8	13.798	0.395	0.769
11	11	63522	1:08:30.22	-73:05:13.3	12.777	0.222	1.203
12	11	77218	1:07:54.31	-72:40:58.7	12.976	-0.381	0.554
13	11	15501	1:08:54.79	-72:24:52.0	13.620	0.384	0.772

Table 2
Candidate binaries in the LMC

	field	number	RA	DEC	V	B-V	V-I
1	3	79892	5:27:54.83	-69:39:32.6	13.614	-0.098	0.555
2	4	52814	5:26:39.03	-69:25:25.4	13.300	0.611	1.118
3	6	14228	5:20:39.59	-69:19:31.2	13.284	0.900	1.485
4	6	69953	5:22:39.40	-69:57:12.3	13.410	0.169	0.666
5	7	95146	5:19:24.33	-69:25:45.9	13.765	1.326	1.683
6	8	15413	5:15:06.94	-69:35:54.2	13.964	0.350	1.608
7	9	88658	5:14:02.12	-69:39:56.1	13.691	1.712	1.914
8	11	62232	5:08:18.31	-68:46:47.2	13.652	0.782	1.132
9	11	13943	5:09:36.47	-69:04:54.7	13.796	1.666	1.931
10	14	50495	5:03:02.40	-68:47:20.5	13.639	1.197	1.461
11	15	2	5:00:03.03	-69:30:08.6	13.574	1.229	1.536
12	19	89862	5:43:12.33	-70:17:32.3	12.600	0.362	1.036

T a b l e 1
Candidate binaries in the SMC

	field	number	RA	DEC	V	B-V	V-I
1	4	16915	0:47:08.72	-73:14:11.5	13.057	0.725	1.197
2	5	19933	0:50:32.09	-72:52:09.3	13.695	0.370	0.873
3	6	17257	0:51:22.85	-73:15:41.8	13.462	-0.283	0.228
4	6	35446	0:51:45.43	-73:04:59.7	12.719	0.379	0.789
5	6	10522	0:52:19.06	-73:09:22.7	13.342	0.673	1.035
6	6	50956	0:53:44.49	-72:33:19.0	13.294	1.377	1.688
7	6	11169	0:54:09.53	-72:41:42.9	13.706	0.392	1.082
8	9	14255	1:02:37.90	-72:35:54.4	13.386	1.252	1.525
9	10	545	1:05:10.31	-72:16:44.4	13.683	1.425	1.766
10	11	53227	1:07:04.55	-72:25:51.8	13.798	0.395	0.769
11	11	63522	1:08:30.22	-73:05:13.3	12.777	0.222	1.203
12	11	77218	1:07:54.31	-72:40:58.7	12.976	-0.381	0.554
13	11	15501	1:08:54.79	-72:24:52.0	13.620	0.384	0.772

T a b l e 2
Candidate binaries in the LMC

	field	number	RA	DEC	V	B-V	V-I
1	3	79892	5:27:54.83	-69:39:32.6	13.614	-0.098	0.555
2	4	52814	5:26:39.03	-69:25:25.4	13.300	0.611	1.118
3	6	14228	5:20:39.59	-69:19:31.2	13.284	0.900	1.485
4	6	69953	5:22:39.40	-69:57:12.3	13.410	0.169	0.666
5	7	95146	5:19:24.33	-69:25:45.9	13.765	1.326	1.683
6	8	15413	5:15:06.94	-69:35:54.2	13.964	0.350	1.608
7	9	88658	5:14:02.12	-69:39:56.1	13.691	1.712	1.914
8	11	62232	5:08:18.31	-68:46:47.2	13.652	0.782	1.132
9	11	13943	5:09:36.47	-69:04:54.7	13.796	1.666	1.931
10	14	50495	5:03:02.40	-68:47:20.5	13.639	1.197	1.461
11	15	2	5:00:03.03	-69:30:08.6	13.574	1.229	1.536
12	19	89862	5:43:12.33	-70:17:32.3	12.600	0.362	1.036